The Eighth Asia-Pacific Conference on Wind Engineering,
December 10–14, 2013, Chennai, India

NUMERICAL STUDY ON THE EFFECT OF FLAP ON VORTEX-INDUCED VIBRATION OF BOX SECTION OF A BRIDGE

Anh Dat Tran[1], Hiroshi Katsuchi[2], Hitoshi Yamada[3], Mayuko Nishio[4].
[1]*Doctoral Student of Civil Engineering, Yokohama National University, Japan, tran-anh-cv@ynu.ac.jp*
[2]*Professor of Civil Engineering, Yokohama National University, Japan, katsuchi@ynu.ac.jp*
[3]*Professor of Civil Engineering, Yokohama National University, Japan, y-yamada@ynu.ac.jp*
[4]*Associate Professor of Civil Engineering, Yokohama National University, Japan, nishio@ynu.ac.jp*

ABSTRACT

In this paper, numerical analysis with Reynolds Average Navier-Stokes (RANS) equations based $k-\varepsilon$ model is performed to investigate the role of flap as a countermeasure to vortex-induced oscillation of a box section of a bridge. Mean values of force coefficients of basic box section are first compared with experimental results from a wind tunnel to ensure the reliability of numerical simulation. The effect of flap on vortex-induced oscillation of a box section is studied by changing the angle of flap and the gap between barrier and flap. The power spectrum density (PSD) of velocity at the wake region is obtained in order to evaluate the fluctuations in the intensity of vortex shedding behind box section. Thereafter, the PSD of lift coefficient derived from different flap simulations manifests the influence of shape of flap on wind flow distribution pattern. In addition, the root mean square (RMS) of pressure coefficient along the perimeter of section as well as the flow pattern visualization are expressed to comprehend the flow characteristics around box section and the vortex-induced vibration suppressing mechanism in the presence of flap with its many distinct configurations. Finally, the recommendation on application of flap for a box section is given to reduce the amplitude of vortex-induced oscillation.

Keywords: Computational fluid dynamics (CFD), Box section, Flap, Reynolds Average Navier-Stokes model (RANS), Vortex-induced vibration

1. Introduction

Long span bridges are very sensitive to the impact of wind load. The destruction of Tacoma Narrows Bridge by wind effects in 1940 is a typical instance of the violation in ultimate limit state. If the oscillation of components of bridge exceeds the allowable amplitude of serviceability limit state, the safety of bridge must be considered adequately, its example is Trans-Tokyo Bay Bridge which was utilized the suppressing method over vortex-induced vibration. Therefore, study on the effect of wind on long span bridges has always played an important role. Under the influence of wind load, the safety of long span bridges must be thoroughly investigated to not only satisfy ultimate limit state, but also meet fully requirements of serviceability state.

Box bridge section has been often used in long span bridges because of its own advantages. In design process, the shape of box section is decided on variety conditions and its optimal aerodynamic stable characteristics have not been reached. As a consequence, it leads to aerodynamic instability phenomena of span structure or the excess of allowable limitation amplitude. Aerodynamic countermeasures are often considered to attach to cross-section as suppressing solution for the vibrations instead of modifying the configurations of original box section. They include many different types. Each one has numerous geometrical configurations. Moreover, a small modification in geometry of countermeasures can cause the large change of flow. Normally, the aero-elastic response of long span bridge girder is examined through wind tunnel tests. The effective countermeasures have primarily been selected on the experiments. Expensive time has lasted case by case with regard to each

Proc. of the 8th Asia-Pacific Conference on Wind Engineering – Nagesh R. Iyer, Prem Krishna, S. Selvi Rajan and P. Harikrishna (eds)
 Published by Research Publishing, Singapore. ISBN: 978-981-07-8011-1
doi:10.3850/978-981-07-8012-8_140

countermeasure and various positions of one particular type as well. In the other hand, the experimental models in wind tunnel do not support sufficient information to explain mechanism of wind flow.

Nowadays, numerical study has become a useful tool in wind engineering. The interaction between a structure and wind flow is being frequently analyzed using sophisticated numerical simulations. The results from computational fluid dynamic (CFD) models are getting closer to experimental investigations. The amount of researches using numerical simulations related to aerodynamic countermeasures attached to the bridge section has increased remarkably in the past decade due to the construction of large number of long span bridges. Lee et al. (1997) promulgated the investigations on the vortex-induced vibration of Seohae Bridge section using RANS turbulent model. In addition, aerodynamic study of slotted box girder using Large Eddy Simulations (LES) was reported by Watanabe and Fumoto (2008). Recently, numerical study on suppression of vortex-induced vibrations of box girder bridge section by aerodynamic countermeasures was carried out by Sarwar and Ishihara (2010). In this study, the reliability of 3D LES turbulent model for the vortex-induced vibration prediction in the presence of aerodynamic countermeasures was affirmed in comparison with the experimental results. Sarwar and Ishihara also concluded that use of double flaps decreases the vortex formation, whereas use of fairings results in a strong vortex formation on the upper surface of box girder section which rather leads to a larger amplitude of vibration.

This paper focuses on the effect of flap in reducing the amplitude of vortex-induced oscillation of a box section through CFD simulations. Its aim is to understand the mechanism of wind flow around the box section in the presence of flap. The flaps are simulated with many different gaps and angles. This study uses RANS simulation with $k-\varepsilon$ model. The RMS of pressure coefficient along the perimeter of box section, the PSD of lift coefficient, the PSD of velocity at the wake region and the flow pattern are presented to illustrate the influence of different configurations of flap. Subsequently, the recommendation on application of flap to suppress vortex-induced oscillation of a box bridge section is presented.

2. Numerical Simulations

Numerical simulations use RANS equations where all of the unsteadiness is averaged out to approach turbulence. The $k-\varepsilon$ model is utilized to close governing equations. The finite volume method was used for the discretization. This study employs STAR-CCM+ software as solver.

2.1. Governing Equations

The governing equations used RANS model for incompressible flows without body forces can be written in tensor notation and Cartesian coordinates as:

$$\frac{\partial(\rho\overline{u_i})}{\partial x_i} = 0 \tag{1}$$

$$\frac{\partial(\rho\overline{u_i})}{\partial t} + \frac{\partial}{\partial x_j}(\rho\overline{u_i}\,\overline{u_j} + \rho\overline{u_i'u_j'}) = -\frac{\partial\overline{p}}{\partial x_i} + \frac{\partial\overline{\tau}_{ij}}{\partial x_j} \tag{2}$$

where $\overline{u_i}$, $\overline{u_j}$ and $\overline{p}$ are mean velocities and pressure. The term of $\rho\overline{u_i'u_j'}$ is called the Reynolds stresses. The $\partial\overline{\tau}_{ij}$ are the mean viscous stress tensor components:

$$\partial\bar{\tau}_{ij} = \mu\left(\frac{\partial\overline{u_i}}{\partial x_j} + \frac{\partial\overline{u_j}}{\partial x_i}\right) \tag{3}$$

The $k-\varepsilon$ turbulence model is used to close the above equations. In this model, the transport equation for turbulent kinetic energy k and the transport equation for dissipation of turbulent kinetic energy ε are depicted as following, respectively:

$$\frac{\partial(\rho k)}{\partial t} + \frac{\partial(\rho\overline{u_j}k)}{\partial x_j} = \frac{\partial}{\partial x_j}(\mu\frac{\partial k}{\partial x_j}) - \frac{\partial}{\partial x_j}(\frac{\rho}{2}\overline{u_j'u_i'u_i'} + \overline{p'u_j'}) - \rho\overline{u_i'u_j'}\frac{\partial\overline{u_i}}{\partial x_j} - \mu\frac{\overline{\partial u_i'\partial u_i'}}{\partial x_k\partial x_k} \tag{4}$$

$$\frac{\partial(\rho\varepsilon)}{\partial t} + \frac{\partial(\rho u_j\varepsilon)}{\partial x_j} = C_{\varepsilon 1}P_k\frac{\varepsilon}{k} - \rho C_{\varepsilon 2}\frac{\varepsilon^2}{k} + \frac{\partial}{\partial x_j}(\frac{\mu_t}{\sigma_\varepsilon}\frac{\partial\varepsilon}{\partial x_j}) \tag{5}$$

The eddy viscosity and the constants for model are expressed as:

$$\mu_t = \rho C_\mu\sqrt{k}L = \rho C_\mu\frac{k^2}{\varepsilon} \tag{6}$$

$$C_\mu = 0.09; C_{\varepsilon 1} = 1.44; C_{\varepsilon 2} = 1.92; \sigma_k = 1.00; \sigma_\varepsilon = 1.30 \tag{7}$$

2.2. Analysis Conditions

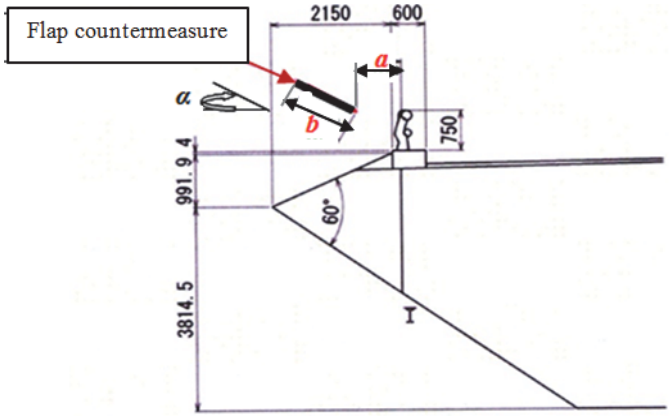

Fig. 1 Geometry configurations of box girder and flap

Fig. 1 particularly shows the geometry configurations of the box section. The representative dimensions of box section are the width B between two edges of section and the depth D between the upper and lower surfaces at center girder. The aspect ratio between B and D of section is 3.20. The other analytical conditions are summarized in Table 1.

Table 1: Dimension and analysis conditions

Parameter	Units	Value
Width (B)	(m)	0.30
Depth (D)	(m)	0.094
Aspect Ratio (B/D)		3.20
Number of elements		140,000-150,000
Reynolds number		10,000
Scale		1/50
Time step (Δt)	(s)	0.0005

The barrier of girder is set up in simulations to examine its influence to flow pattern. The characteristics of flap are varied by changing the length (b), the gap (a) and the angle (α).

2.3. Analysis Domain, Meshing and Boundary Conditions

The width and depth of analysis domain are 20D and 40D, respectively. Fine mesh is used in the vicinity of the section and coarser mesh is set at the areas far from section. The non-slip boundary is assigned at the perimeter of section, top and bottom wall corresponding to the conditions in wind tunnel tests. Fig. 2 describes in detail about the analysis domain, meshing size and boundary condition.

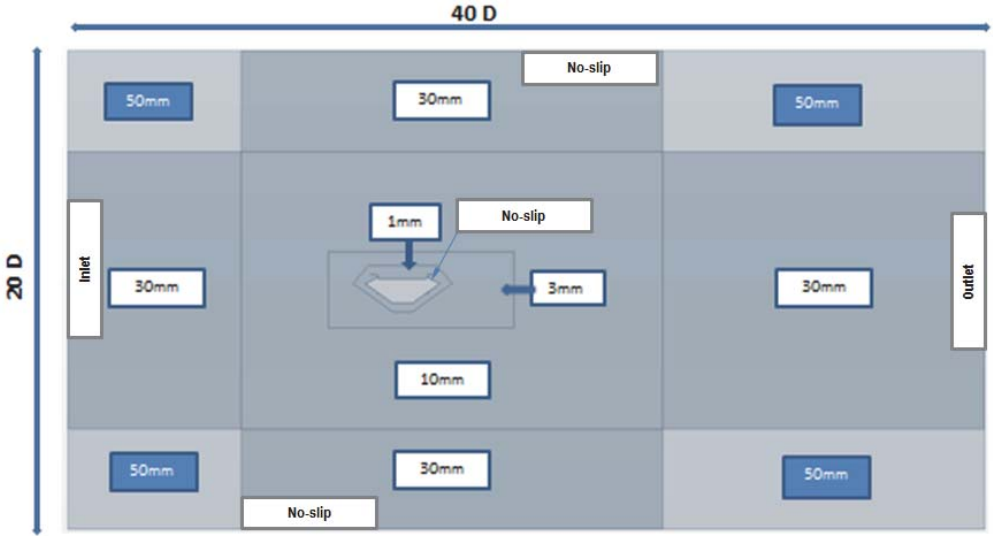

Fig. 2 Analysis domain, meshing size and boundary conditions

3. Results and Discussions

3.1. Mean values of force coefficients of basic box section

Drag force F_D, lift force F_L and pitching moment M on box section (per unit of span) can be rendered dimensionless in terms of drag coefficient C_D, lift coefficient C_L and moment coefficient C_M, respectively. These coefficients are expressed as follows:

$$C_D = \frac{F_D}{\frac{1}{2}\rho U^2 D} \tag{8}$$

$$C_L = \frac{F_L}{\frac{1}{2}\rho U^2 B} \tag{9}$$

$$C_M = \frac{M}{\frac{1}{2}\rho U^2 B^2} \tag{10}$$

where ρ is air density, U is mean oncoming velocity, D and B are representative dimensions of box girder section.

Definition of the above forces and the angle of attack of wind flow are shown in Fig. 3. The along-flow direction of F_D, upward direction of F_L and clockwise direction of M are conventionally positive directions.

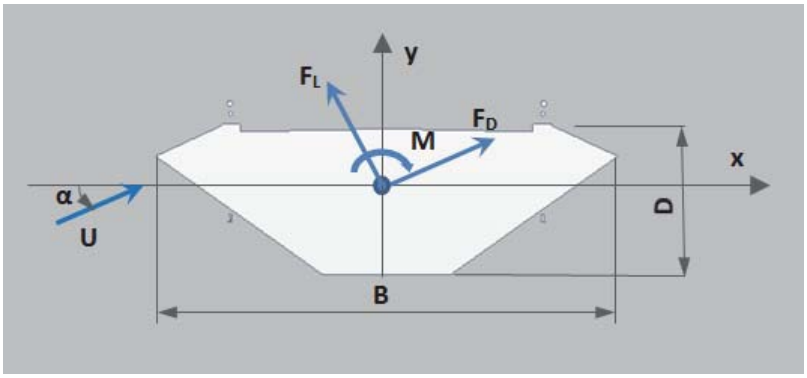

Fig. 3 Definitions of direction of forces and angle of attack

Numerical analysis simulations are checked in terms of comparison with three force coefficients from wind tunnel tests of basic section at several angles of attack. Fig. 4 shows that the obtained values have agreed with the experimental ones to prove the reliability of numerical simulations.

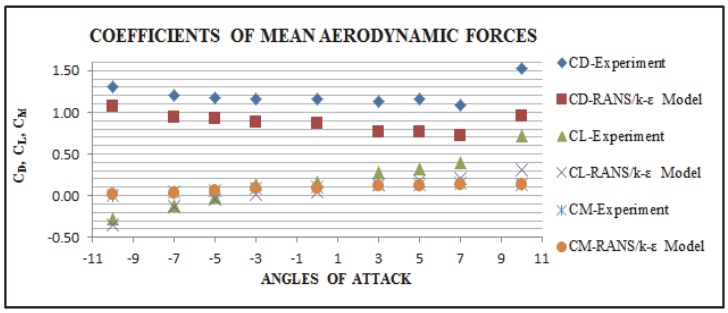

Fig. 4 Coefficients of mean aerodynamic forces of basic box section

3.2. Effect of flap to suppress vortex-induced vibration

The investigations on the effect of flap to suppress vortex-induced vibration are presented in this section. The examinations relating to the aerodynamic characteristics are performed to determine the influence of geometrical modifications of flap. First, the PSD of velocity at wake region and the PSD of lift coefficient are mentioned. Then, the RMS of pressure coefficient along the perimeter of section and the flow pattern visualization are verified.

3.2.1. Velocity of wake flow and unsteady lift force

In numerical simulations, the velocity of wake flow is measured a point A located at (D; D/2) downstream the model section. The investigations include many cases in which the length, the gap and the angle of flap are increased such as 1000/600/0, 1000/600/10, 1000/600/30, 1000/800/0, 1000/800/10, 1000/800/30, 1500/800/30 and 1000/1300/30 (length/gap/angle).

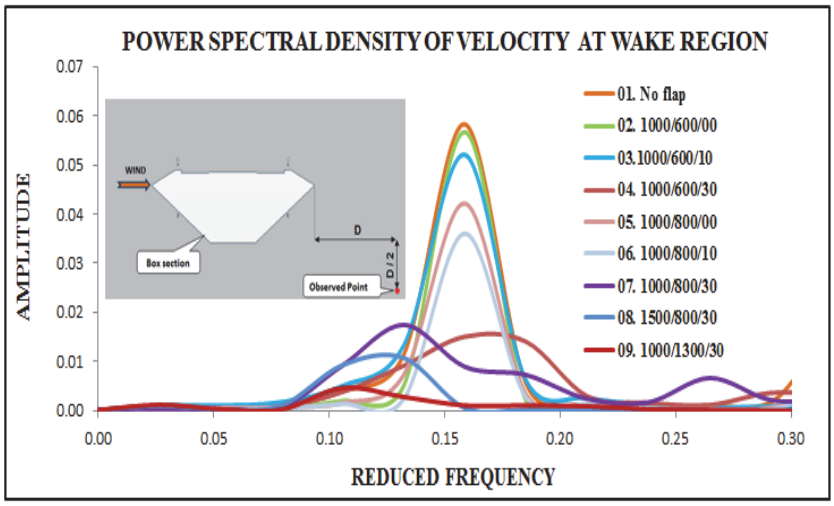

Fig. 5 PSD of velocity at wake region

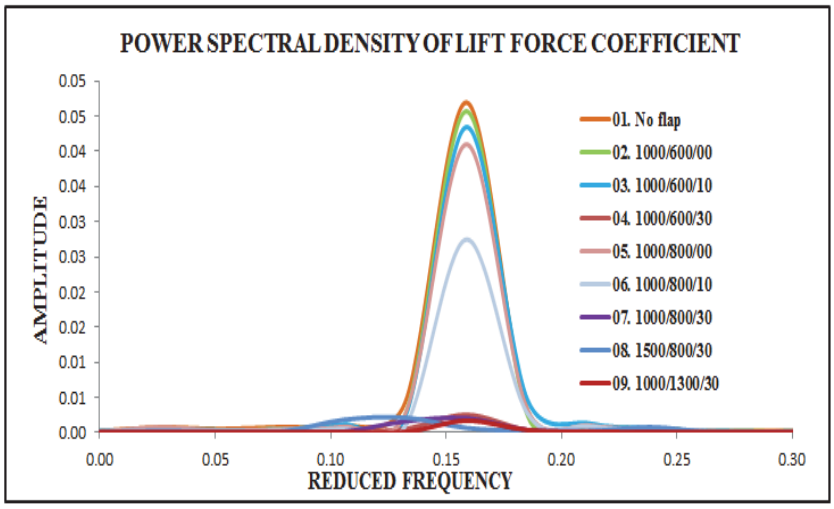

Fig. 6 PSD of lift coefficient

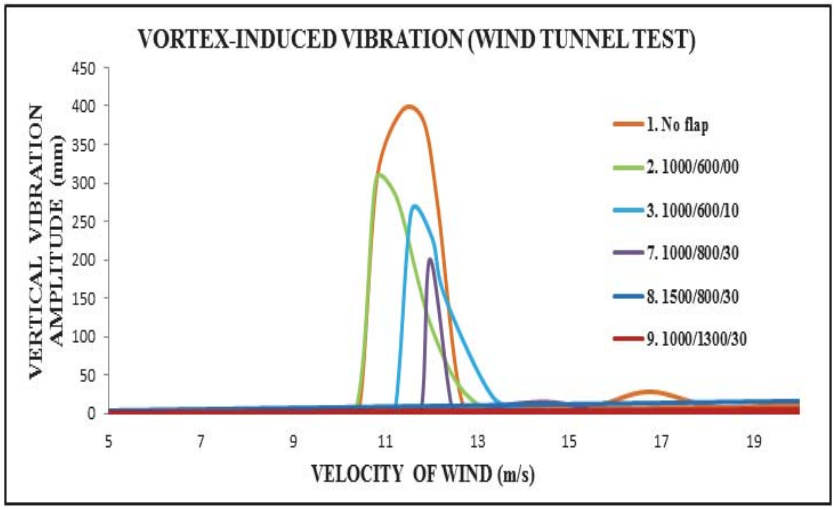

Fig. 7 Vortex-induced vibration amplitude from wind tunnel tests

The PSD of velocity of wake flow shows that it gains the maximum value for the basic box section and gradually decreases for the box section with flap attached as is shown in Fig. 5. When the angle and the gap of flap increase, the value of it becomes smaller for the cases such as 1000/600/30 and 1000/800/30. Its decrement is also found if the 30^o angle of flap is kept, while the length and gap of flap are modified to be longer, such as the cases of 1500/800/30 and 1000/1300/30. Besides, the change of the gap of flap does not lead a strong variation, whereas the modification of the angle of flap brings in considerable results. The effective flap can be found by the combination between them.

The PSD of lift coefficient has the same performance and is shown in Fig. 6. It also has the largest value for the basic box section and the 30^o angle of flap results in the low value of PSD. Therefore, they demonstrate the effect of flap on box section in the intensity reduction of vortex shedding behind box section. The presence of flap with appropriate configurations will redistribute the flow pattern and diminish the fluctuation of flow around the box girder.

The experimental results in wind tunnel for the same circumstances have close agreement with the values as reported above by means of the measured vortex-induced vibration amplitudes is depicted in Fig. 7. The reliability of CFD simulations is affirmed once more.

3.2.2. RMS of pressure coefficient on the surface of box section and flow pattern around it

The RMS value of pressure coefficient is the square root of the arithmetic average of the square of the fluctuating pressure coefficient. In the case of a set of n fluctuation values, the value of RMS is expressed as follows:

$$RMS_C = \sqrt{\frac{c_1^2 + c_2^2 + ... + c_n^2}{n}} \tag{11}$$

where $c_1, c_2, ..., c_n$ are the fluctuations of pressure coefficient C.

The time history of pressure coefficient is obtained at points along the perimeter of box section in numerical simulations. Then, the value of RMS is calculated as formula (11). The distribution of it around the box section is drawn in Fig. 8 for the cases of basic section, 1000/800/00, 1000/800/10 and 1000/800/30 flap. It shows that the RMS has largest value for the case of basic box section. In cases of flap attached, the RMS has higher value when the angle of flap approaches to 0 degree. The RMS of 30^o angle of flap has smaller value in comparison with the value of other cases. Consequently, the presence of suitable flap plays an important role to reduce the fluctuation of pressure coefficient on the surface of box girder section.

To comprehend the characteristics of flow around the box section, the flow visualization is given. Fig. 9 depicts the flow pattern around the box section for the cases of basic section, 1000/800/0, 1000/800/10 and 1000/800/30 flap to investigate the mechanism of wind flow. There, if the gap and angle have a sufficiently large value, the flow will be intercepted by flap and go down stronger to the upper surface of faring. The combination between the fairing of box section and suitable flap plays an important role in controlling wind flow to be smoother at the wake region. It controls the vortex formation in the wake region as vortices become more regular and it reduces the amplitude of vortex-induced oscillation. This phenomenon will not occur with the horizontal flap, insufficient gap and angle.

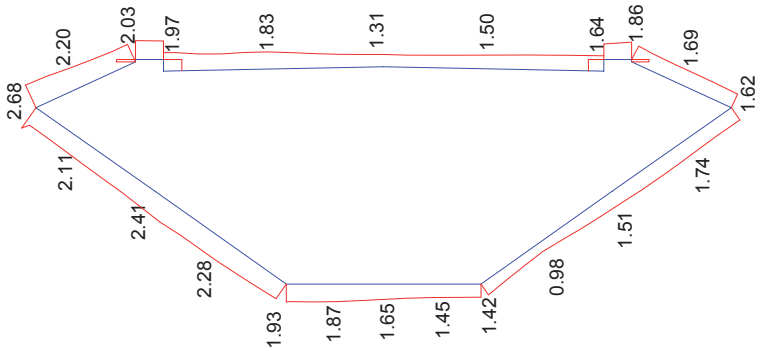

a. Basic box section

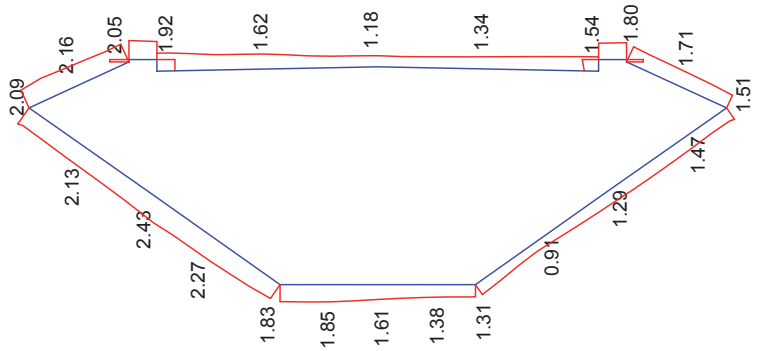

b. 1000/800/00 flap

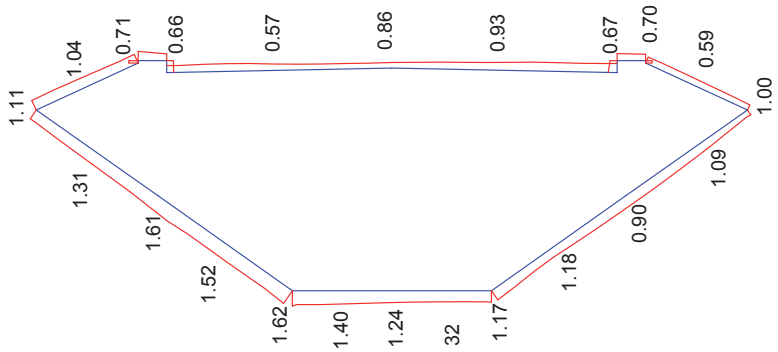

c. 1000/800/10 flap

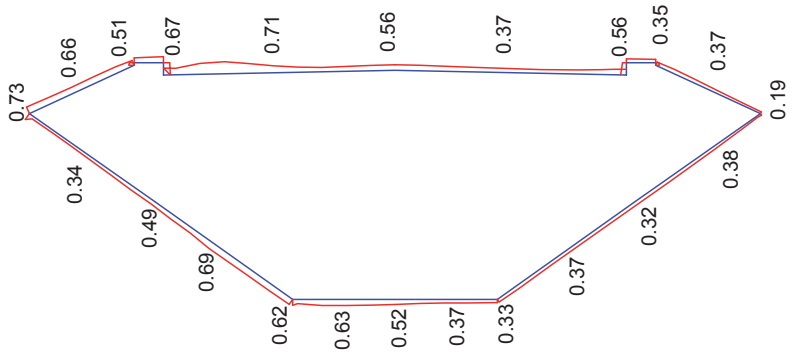

d. 1000/800/30 flap

Fig. 8 Distribution of RMS of pressure coefficient on the surface of box section

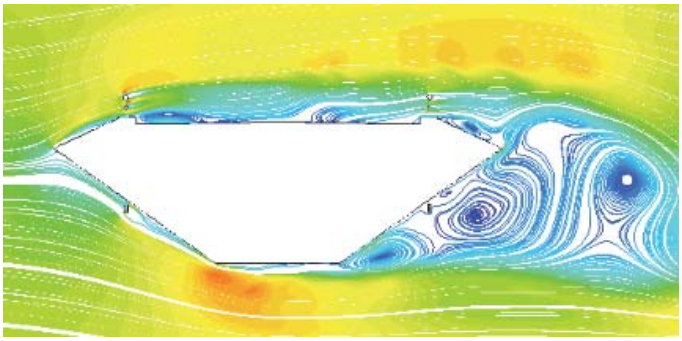

a. Basic box section

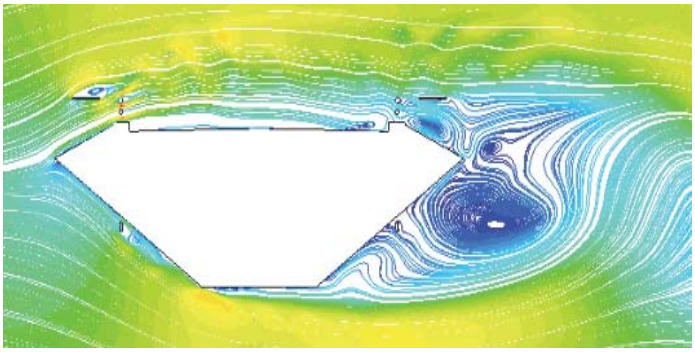

b. 1000/800/00 flap

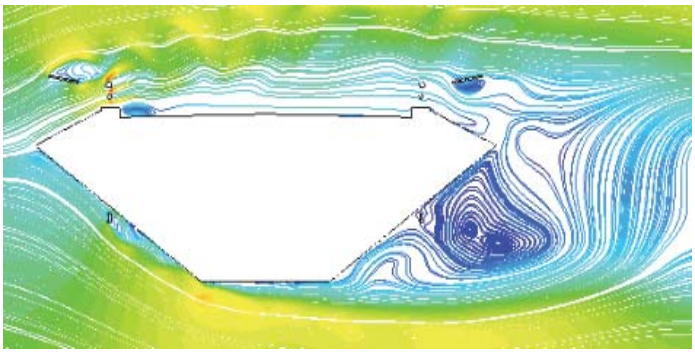

c. 1000/800/10 flap

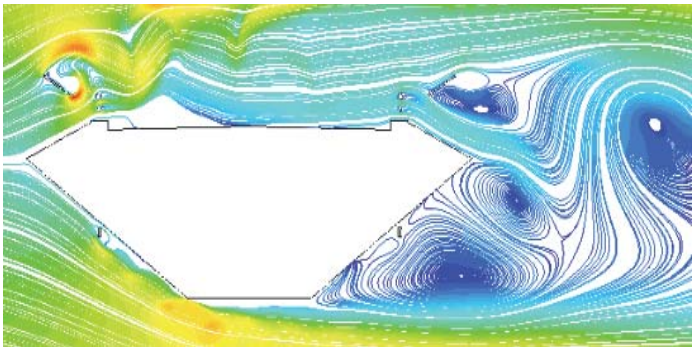

d. 1000/800/30 flap

Fig. 9 Wind flow pattern around the box section

4. Conclusions

Numerical analysis CFD using RANS based on $k-\varepsilon$ model obtained in this paper has led a good agreement to the experimental results from wind tunnel tests. The presence of flap on box girder section has resulted in change of wind flow distribution and has brought the meaningful effect in diminishing vortex-induced oscillation amplitude. It is showed that use of horizontal flap and insufficient gap do not lead to lessen remarkably the rousing flow at leeward area. However, the combination between the fairing of box section and suitable flap plays an important role in controlling wind flow to be smoother at the wake region. Based on results of numerical study, the PSD of velocity at leeward zone and the PSD of lift coefficient manifested the important effect of inclination angle and gap of flap. Besides, the flow pattern and the RMS of pressure coefficient on section supplied comprehensive investigation the flow mechanism with many distinct geometrical characteristics of flap. Thence, flap with sufficiently large gap and angle is recommended to suppress the vortex-induced vibration amplitude of box section under wind load.

References

Francesco, R., Enrico, T., Horia, H. (2002), "Pressure Distribution, Aerodynamic Forces and Dynamic Response of Box Bridge Sections", Journal of Wind Engineering and Industrial Aerodynamics 90, pp. 1135-1150.

Katsuchi, H. (2012), "Wind Tunnel Experiments Report of Ohashi Shinminato Bridge", Yokohama National University (in Japanese).

Sarwar, M.W., Ishihara, T. (2010), "Numerical Study on Suppression of Vortex-induced Vibrations of Box Girder Bridge Section by Aerodynamic Countermeasures", Journal of Wind Engineering and Industrial Aerodynamics 98, pp. 701-711.

Simiu, E and Scanlan, R. H. (1996), Wind Effects on Structures, 3rd Edition, John Wiley & Sons, New York, USA.